Derivation of Birmingham's summer surface urban heat island from MODIS satellite images

Tomlinson, Charlie; Chapman, Lee; Thornes, John; Baker, Christopher

DOI:
10.1002/joc.2261

INTERNATIONAL JOURNAL OF CLIMATOLOGY
Int. J. Climatol. **32**: 214–224 (2012)
Published online 3 December 2010 in Wiley Online Library
(wileyonlinelibrary.com) DOI: 10.1002/joc.2261

Derivation of Birmingham's summer surface urban heat island from MODIS satellite images

C. J. Tomlinson,[a]* L. Chapman,[b] J. E. Thornes[b] and C. J. Baker[a]
[a] *School of Civil Engineering, University of Birmingham, Edgbaston, Birmingham, B15 2TT, UK*
[b] *School of Geography, Earth and Environmental Sciences, University of Birmingham, Edgbaston, Birmingham, B15 2TT, UK*

ABSTRACT: This study investigates the summer (June, July, August) night urban heat island (UHI) of Birmingham, the UK's second most populous city. Land surface temperature remote sensing data is used from the MODIS sensor on NASA's Aqua satellite, combined with UK Met Office station data to map the average variation in heat island intensity over the Birmingham conurbation. Results are presented of average UHI events over four Pasquill-Gifford stability classes D, E, F, and G between 2003 and 2009, as well as a specific heatwave event in July 2006. The results quantify the magnitude of the Birmingham surface UHI as well as the impact of atmospheric stability on UHI development. During periods of high atmospheric stability, a UHI of the order of 5 °C is evident with a clear peak in the central business district. Also identified, are significant cold spots in the conurbation. In one city park, recorded surface temperatures are up to 7 °C lower than the city centre. Copyright © 2010 Royal Meteorological Society

KEY WORDS urban heat island; MODIS; remote sensing; GIS; Birmingham; surface temperatures

Received 1 April 2010; Revised 13 September 2010; Accepted 19 October 2010

1. Introduction

1.1. Urban heat islands

The urban heat island (UHI) is an extensively studied phenomenon and refers to the difference in temperature between a conurbation and the surrounding rural area. There are many factors that contribute to the formation of the UHI. Urban geometry is often cited as the main cause (Oke, 1987), and is frequently parameterised in terms of the sky view factor (Bradley *et al*., 2002; Svensson, 2004, Unger, 2004) or surface volume compactness (Unger, 2006). Other major influences include the density and population of a conurbation (Oke, 1987) and its associated anthropogenic heat release (Smith *et al*., 2009), alongside landuse and vegetation cover (Stabler *et al*., 2005) which affect albedo, emissivity, and surface roughness. The cumulative effect of these factors can result in a maximum UHI of significant magnitude, such as the 7 °C measured in London (Watkins *et al*., 2002) or greater than 8 °C in New York City (Gedzelman *et al*., 2003).

A number of review papers illustrate the significant progress that has been made in the study of the UHI phenomenon, in particular, improving the nature and accuracy of measurements, and the development of models (Arnfield, 2003; Mckendry, 2003; Arnfield, 2005, 2006; Souch and Grimmond, 2006). However, despite the broad research effort, an area of research which still requires attention is the inclusion of the UHI phenomenon in climate models. Indeed, a UHI component is notably absent in many models, including the UK Met Office Hadley Centre Regional Climate Model (RCM) which has been used in the UK Climate Programme for both the UKCIP02 (Gawith *et al*., 2009) and UKCP09 (Jenkins *et al*., 2009) climate change projections. Including the UHI effect in climate models would improve the accessibility of climate data for planners (Gawith *et al*., 2009), and high-resolution measurements of UHI effects would be a useful input for model development and validation. This paper aims to produce a simple and transferable technique to quantify the average surface UHI in Birmingham, UK, which could be used by urban planners in conjunction with climate change scenarios, for example, relating to future health risk work and when making planning decisions at the neighbourhood scale.

Traditional measurements of the near-surface UHI are often made using pairs or urban/rural weather stations (Kukla *et al*., 1986; Karl *et al*., 1988) or air temperature transects (Johnson, 1985; Torok *et al*., 2001). However, due to a paucity of high-resolution air temperature measurements in most cities, high-resolution studies are limited to the measurement of surface temperatures and hence, the surface or 'skin' UHI as measured by satellites (Streutker, 2003). Surface temperatures are far easier to obtain due to the availability of products such as the thermal land surface temperature (LST) data from the Moderate Resolution Imaging Spectroradiometer (MODIS) instrument onboard the National Aeronautics and Space Administration's (NASA) Aqua (EOS-PM1) or Terra

* Correspondence to: C. J. Tomlinson, School of Civil Engineering, University of Birmingham, Edgbaston, Birmingham, B15 2TT, UK. E-mail: cjt512@bham.ac.uk

(EOS-AM1) satellites. It is important to note that the relationship between air and surface temperature is not fully understood, and discussions (Arnfield, 2003; Weng, 2009) refer to both studies that report similarities (Nichol, 1994), and those that report differences (such as Weller and Thornes, 2001). In this paper, the surface UHI is investigated and no direct relationship to air temperature is suggested or inferred.

1.2. Thermal satellite remote sensing techniques

Satellite techniques for UHI measurement were first investigated in the 1970s (Matson *et al.*, 1978; Price, 1979), but as comparisons between review papers by Gallo *et al.* (1995) and Weng (2009) illustrate, the field is rapidly changing and advancing.

The increased spatial coverage that satellite remote sensing techniques can provide in comparison to weather station data (Mendelsohn *et al.*, 2007) is the main reason the technique is chosen for many studies of urban climate. Multiple studies have explicitly mentioned the potential and usefulness of the MODIS LST product in UHI research (Rajasekar and Weng, 2008; Cheval *et al.*, 2009). In particular, the instantaneous observations, global coverage and promising quality of MODIS data is extremely valuable (Jin and Shepherd, 2005). Although MODIS has been operating on the Aqua satellite since 2002, it is only recently that a sufficient archive of data is freely available for analysis. It is for this reason why there is a limited amount of studies presently available in the literature that explicitly use MODIS data as a tool for urban climatology.

Compared to potential alternatives such as the Advanced Spaceborne Thermal Emission and Reflection Radiometer (ASTER) sensor or Landsat Thermal Mapper (TM)/Enhanced Thermal Mapper Plus (ETM+), the MODIS LST product is considered a coarse resolution ($\sim$1 km) dataset. However, the high temporal resolution (twice daily per satellite) of MODIS makes it ideal for UHI studies. In comparison, the number of images available from ASTER or Landsat is significantly less than MODIS.

The MODIS LST product has already been used for surface UHI investigations in many countries and cities of varying sizes and scales across the globe (Jin *et al.*, 2005). Notable studies include Hung *et al.* (2006) who used MODIS to quantify the UHI in eight Asian megacities, and Pongracz *et al.*, (2006) who conducted a similar study on the ten most populated cities of Hungary. However, the most relevant study for this paper is recent research from Romania where MODIS was used to calculate the average intensity of the UHI in Bucharest for the month of July between 2000 and 2006 (Cheval and Dumitrescu, 2009) as well as under heatwave conditions in 2007 (Cheval *et al.*, 2009).

Studies have explicitly pointed out the negative effects the UHI may have on health (Changnon *et al.*, 1995; Rooney *et al.*, 1998; Basu and Samet, 2002; Conti *et al.*, 2005), particularly when combined with heatwave events. The UHI has also been shown to influence air quality (Huang *et al.*, 2005) and atmospheric pollution (Sarrat *et al.*, 2006) among other things. Heat risk studies (Lindley *et al.*, 2006) explicitly mention the lack of a UHI component, despite UHI being described as one of the major problems of the 21st century (Rizwan *et al.*, 2008). For this reason, this study focuses on the summer months of June, July, and August (JJA) as these are more likely to cause a heat health risk due to elevated summer temperatures and heatwaves (Rooney *et al.*, 1998; Basu and Samet, 2002). Furthermore, it has been shown that for temperate cities in the northern hemisphere, such as Birmingham, winter UHIs are smaller in both extents and magnitude than summer equivalents (Hung *et al.*, 2006).

2. Methodology

2.1. Study area

The study area of Birmingham is the second most populous city in the United Kingdom, with an estimated population, in 2007, of over one million (Office for National Statistics, 2009). The extent of the conurbation extends to over approximately 278 km^2, yet despite its size, Birmingham only has one 'urban' weather station (Winterbourne) within the city limits, and one 'rural' weather station (Coleshill) approximately 4.5 km from the eastern edge of the city (Figure 1). Previous research into the Birmingham UHI is limited, partly due to the lack of meteorological stations and data. Unwin (1980) compared urban and rural nocturnal minimum weather station measurements and discovered that the near-surface UHI magnitude could reach 5 °C in settled anticyclonic conditions. Johnson (1985) used a thermograph transect approach from the city centre out through the SW of Birmingham and recorded a maximum near-surface UHI of approximately 4.5 °C during the night. Finally, Bradley *et al.* (2002) used a 1-dimensional energy balance model to calculate a calm clear night surface UHI intensity of 4.7 °C. These few studies contrast with London which has an extensively studied UHI (Watkins *et al.*, 2002; Wilby, 2003; Greater London Authority, 2006; Kolokotroni *et al.*, 2007; Kolokotroni and Giridharan, 2008; Giridharan and Kolokotroni, 2009; Jones and Lister, 2009).

2.2. MODIS data

This study uses the MODIS product MYD11A1 (V5)-MODIS/Aqua Land Surface Temperature and Emissivity Daily L3 Global 1 km Grid SIN. Full technical details are available online and so will not be covered here (Wan, 1999; NASA Land Processes Distributed Active Archive Center, 2009). The MODIS LST product uses split window algorithms and techniques (Wan and Dozier, 1996) that correct for atmospheric effects (including absorption and emission) and surface emissivity (inferred from MODIS land-cover calculations) by utilising multiple bands from the 36 available on the MODIS sensor. This addresses many of the 'traditional' problems associated

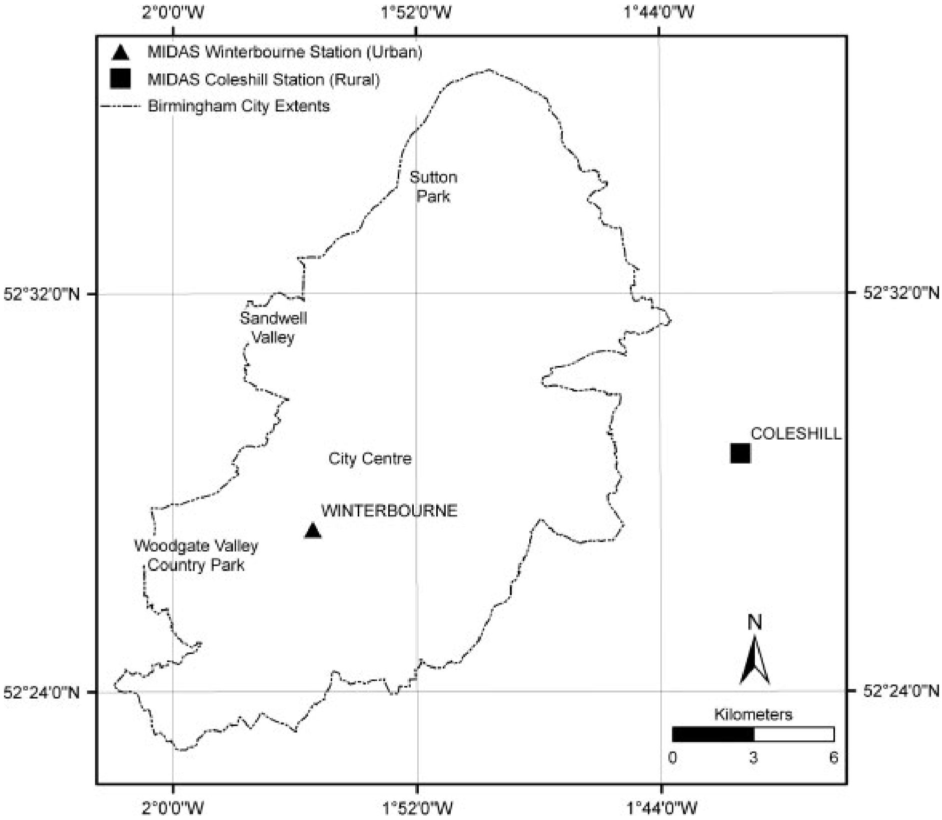

Figure 1. Location of Birmingham, local weather stations, and areas of interest.

with remote sensing measurements of LST, such as emissivity assumptions and unknown or variable atmospheric effects. A number of studies have tested the accuracy of the MODIS LST product with favourable results (Wan, 2002; Wan *et al*., 2004; Coll *et al*., 2005; Wan, 2008).

Although the MODIS sensor is carried on both NASA's Aqua and Terra satellites, only images from Aqua are used for this study as the near-polar sun-synchronous orbit of Aqua resulted in a night image acquisition time for Birmingham at approximately 0130 h local time (compared to approximately 2230 h using Terra). A night image allows a more precise LST calculation as there is no incoming solar radiation to change the surface radiation balance, and nighttime MODIS LST accuracy has been found to be better than day time (Rigo *et al*., 2006). There may be timing differences between air (near-surface) and surface temperature UHI development, but without reliable quantitative evidence the timing of the 0130 h pass seems ideal as Oke, (1987, p. 291) describes maximum air UHI magnitude as 3–5 h after sunset, which in the UK summer is around the time of image acquisition.

Data were obtained for the Birmingham study area over the summer months of June, July, and August (JJA) for the seven-year period between 2003 and 2009, inclusive. Images were batch processed in ESRI ArcMap using the Marine Geospace Ecology Tools (MGET) plugin (Roberts *et al*., 2010). This processing ultimately resulted in a raster file of each image, geo-referenced and trimmed to the study area, with LST converted to degrees Celsius. Quality control of the images was then achieved by selecting only the raster images that contained 100% LST pixel coverage within the extent of the Birmingham conurbation (Figure 1). This last step removed a large amount of the images as MODIS satellite imagery, in common with all thermal infrared sensors, is restricted by cloud cover. The remaining images represented nights with clear skies at the time of the satellite overpass. Indeed, the increased availability of images in the summer months is a major advantage of focussing on the summer UHI. Difficulties in obtaining sufficient images for analysis in winter (Rajasekar and Weng, 2008), due to increased cloud cover (preventing an image being taken) or increased rainfall (causing wet surfaces leading to unreliable LST measurements), is a barrier for research. Other methods such as modelling or microwave remote sensing must be used if high temporal and high spatial LST data is required without the cloud cover limitations imposed by thermal infrared sensors (Wan, 2008).

2.3. MIDAS data

The selected images were classified (Table I.) into Pasquill-Gifford stability classes (Pasquill and Smith, 1983; Sutherland *et al*., 1986; Chapman *et al*., 2001); D (Neutral), E (Slightly Stable), F (Moderately Stable) or G (Extremely Stable) based on the preceding 12-h weather at Coleshill, a WMO weather station 4.5 km east of Birmingham (Figure 1). This weather station was chosen as it is the nearest to the study area which monitors

Table I. Classification of Pasquill-Gifford stability classes (adapted from (Pasquill and Smith, 1983; Chapman *et al.*, 2001)).

Surface wind speed (m s^{-1})	Pasquill-Gifford stability class	
	Night	
	≥4/8 oktas cloud	<4/8 oktas cloud
<2	G	G
2–3	E	F
3–5	D	E
5>	D	D

Table II. Distribution of images and days across Pasquill-Gifford stability classes.

Pasquill-Gifford stability class	Number of days	Number of images
D	73	6
E	123	20
F	65	22
G	60	15
Total	321	63

cloud cover. The Met Office MIDAS WH hourly dataset (UK Meteorological Office, 2006) derived from Coleshill was then used to average the weather for 12 h preceding 0200 h (based on the satellite overpass time ~0130 h) for each image in terms of cloud cover, wind speed, and present weather code (detailing rain or other atmospheric conditions). Present weather codes detailing mist, smoke, haze, cloud, and fog were allowed (10, 04, 05, 01, and 11, respectively) as they can relate directly to local events and have less impact on regional image quality. This allowed the general atmospheric conditions preceding and including image capture to be summarised and further filtered out images that were unsuitable.

This approach resulted in a total of 63 images for analysis, distributed across the 4 Pasquill-Gifford stability classes (Table II.) and 7 years of study (Figure 2). An additional classification of MIDAS data was additionally conducted for all summer (JJA) days over the study period in order to assess the frequency of Pasquill-Gifford classes (Figure 3) over the same 12-h time period.

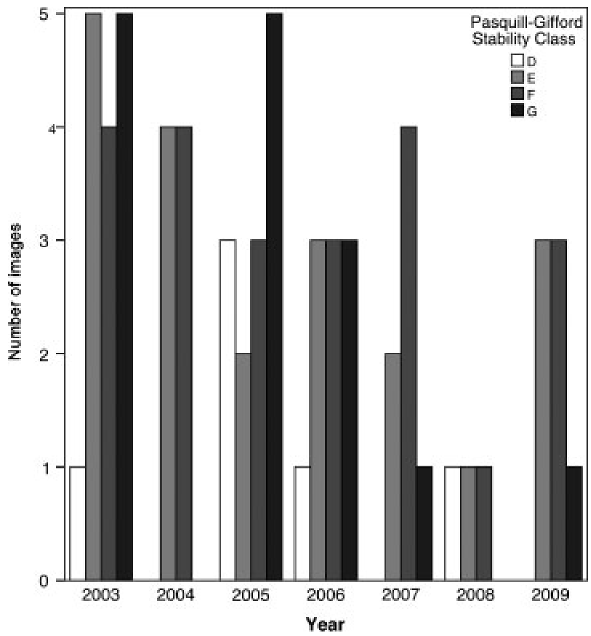

Figure 2. Selected images by Pasquill–Gifford class and year.

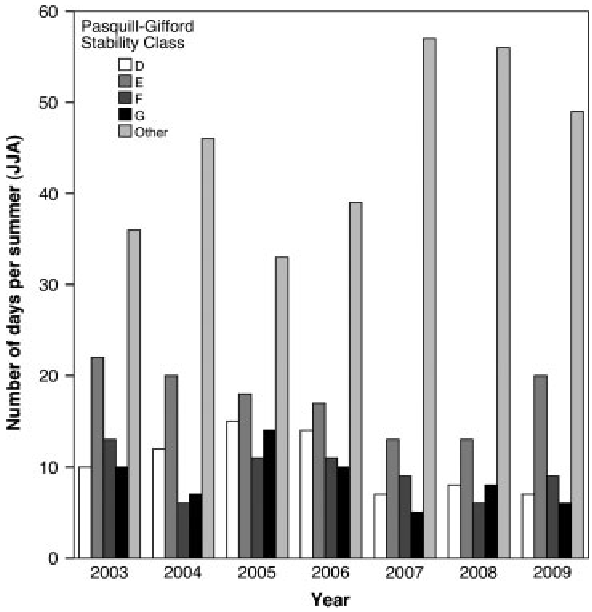

Figure 3. Pasquill-Gifford frequency in summer (JJA) 2003–2009. The 'Other' class refers to days that could not be defined into stability classes D, E, F, or G because of the filtering (detailed in Section 2.3).

2.4. Calculation of UHI magnitude

For each of the four stability classes, spatial averages of LST values were calculated, resulting in a single raster image for each class containing average LST values for each ~1 km cell. The magnitude of the UHI present in each image was calculated by using a rural reference LST value to residualise the temperature value of each pixel across the whole image. Due to its rural location (Figure 1), the rural reference LST value was taken as the satellite LST value for the cell containing Coleshill weather station. Although the use of satellite data gave the possibility for choosing any reference area, Coleshill was chosen in order to help facilitate potential future research comparing MODIS LST and air temperature. This step left four images, one for each Pasquill-Gifford scenario, with values taken to be UHI magnitude, measured as LST difference when compared to Coleshill.

2.5. Land cover data

Finally, in order to investigate the thermal characteristics of differing landuse categories (e.g. Bradley *et al.*, 2002),

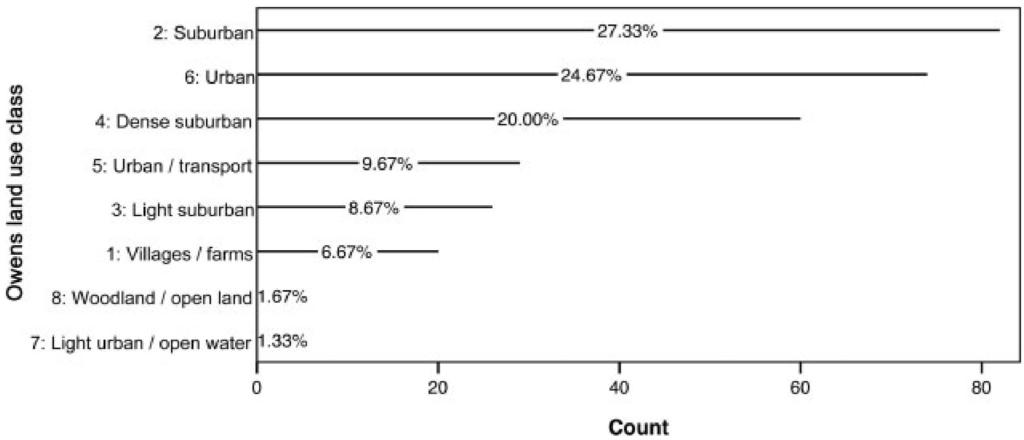

Figure 4. Numerical distribution of Owens land classification across Birmingham.

every pixel in each of the images was categorised with respect to a common landuse schema. Owen *et al*., (2006) derived an 8-category (1 (villages/farms), 2 (suburban), 3 (light suburban), 4 (dense suburban), 5 (urban/transport), 6 (urban), 7 (light urban/open water), 8 (woodland/open land)) urban landuse classification from a principal component analysis and cluster analysis based on data from the Ordnance Survey (national UK mapping agency) and the UK Centre for Ecology and Hydrology. The classification scheme was based on 27 different input attributes and the output is a 1 km^2 grid showing similar urban land morphology. Full details are given in Owen *et al*., (2006). A subset of the whole West Midlands database is used, distributed across Birmingham by frequency (Figure 4) and space (Figure 5). This classification was chosen for a number of reasons. It splits the urban fabric into multiple urban categories, unlike other classifications (including typical satellite land cover classifications) allowing more in-depth comparisons, for example, between different densities of suburbia. Furthermore, it is a similar resolution (1 km^2) to the MODIS data, so minimises problems that could arise when generalising between datasets with large differences in scale.

3. Results and discussion

3.1. Image availability

Table II. details both, the total number of available images used for each of the Pasquill-Gifford class images, as well as the total number of days categorised in each Pasquill-Gifford class over the study period. Here the issue of cloud cover reducing the sample size can clearly be identified as the number of images decreases rapidly between class E and class D due to the increased probability of cloud cover. If cloud cover did not impact image availability, the number of images in class E would be considerably greater as this is the dominant stability class throughout the summer months (Figure 3). Furthermore, exploring the distribution of images by year (Figure 2) it can be seen that whilst classes E and F are present for every study year, the distribution of classes D and G is less regular. Class D is not present in 2004, 2007, or 2009, whilst class G is not present in 2004 and 2008. The UK Met Office seasonal summaries (Met Office, 2010) can help to explain this, for example, 2004 and 2008 summers both had higher than average (1961–1990) rainfall which helps explain the lack of ‘Extremely Stable’ class G images. Similarly, the year 2003 has the most number of images and was associated with a heatwave (Burt, 2004) which implies increased atmospheric stability.

3.2. Atmospheric stability and the Birmingham UHI

The averaged UHI magnitude for the different Pasquill-Gifford stability classes (Figure 6) shows a clear increase in UHI magnitude as atmospheric stability increases. This is expected, and in line with the findings of Morris *et al*., (2001) who show that increases in cloud cover and wind speed reduce UHI magnitude for Melbourne, Australia. When comparing absolute pixel values (Table III.) it can be seen that maximum UHI magnitude (hottest pixel) decreases through the stability classes. Box plots of each scenarios UHI magnitude (Figure 7) agree and show an increase in UHI magnitude as stability increases.

To test for statistical differences between UHI magnitude under the four Pasquill-Gifford classes, the Friedman Analysis of Variance test (ANOVA) was used with post-hoc Wilcoxon Signed Rank tests. These are non-parametric versions of the repeated measures one-way analysis of variance and paired samples Student’s t-test, and were used because the dataset violates assumptions of normality and homogeneity. The results of the Friedman

Table III. Pixel comparison.

	Temperature (°C)				
	Heatwave	G	F	E	D
Hottest pixel	4.88	3.08	2.74	2.27	1.79
Coldest pixel	−2.16	−1.54	−1.39	−0.88	−0.81
Difference	7.04	4.62	4.13	3.15	2.60

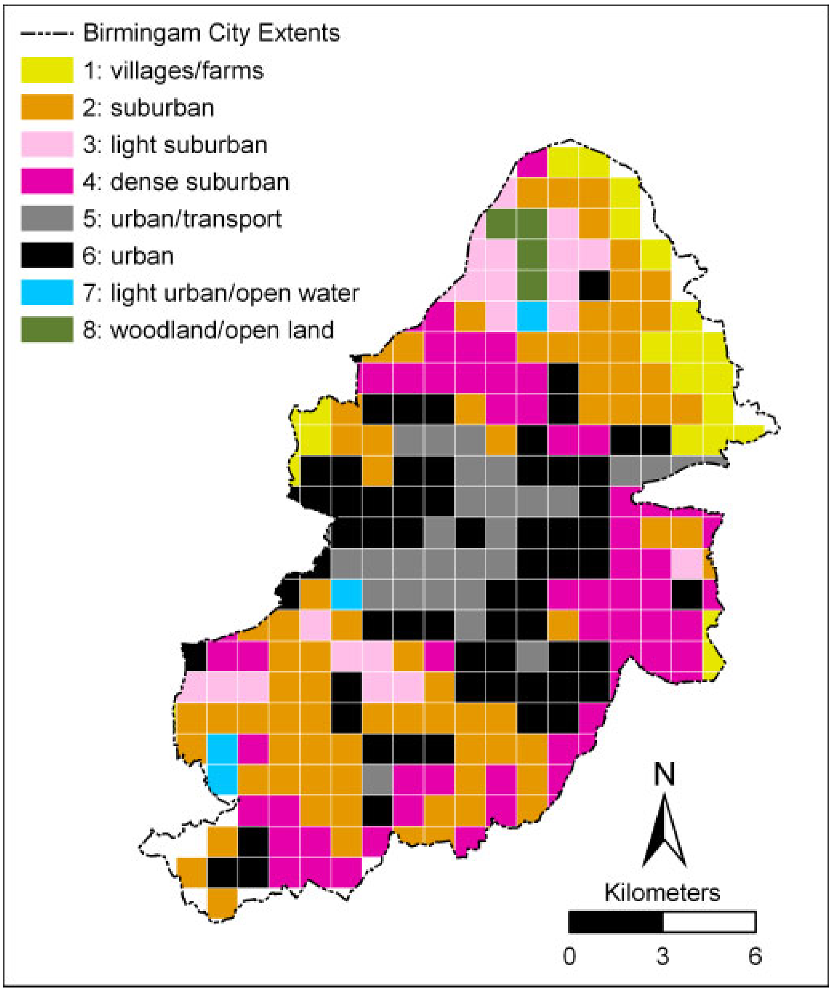

Figure 5. Spatial distribution of Owens land classification across Birmingham. This figure is available in colour online at wileyonlinelibrary.com/journal/joc

ANOVA confirm that significant differences ($p < 0.01$) in UHI magnitude exist between at least two scenarios. The Wilcoxon Signed Rank *post-hoc* tests confirm that significant differences ($p < 0.01$) in UHI magnitude exist between all Pasquill-Gifford changes (D–E, E–F, F–G) when using a Bonferroni-corrected significance level of 0.0033. This significance adds confidence to both the methodology used and the underlying MODIS data as the differences agree with expectations.

Clear spatial trends in temperature are evident in all four images and can be clearly delineated by contour mapping (Figure 6). In general, these trends hold for all stability classes, however, class D (Neutral) shows weaker trends and lower temperatures. The highest temperatures are consistently seen in the city centre of Birmingham, with a UHI magnitude >3, >2.5, >2, and $>1.5\,^{\circ}$C for Pasquill-Gifford classes G, F, E, and D, respectively, with contour mapping at the 0.5 °C interval. Exact LST values are given in Table III. The exact spatial location of the centre of the UHI moves slightly dependant on stability class, but generally the highest UHI magnitude is around the central business district which contains Birmingham New Street Railway station and the main commercial area (Figure 1). In the northwest corner of Birmingham, all stability classes exhibit a significant cold spot, with maximum magnitudes of <-1.5, <-1, <-0.5, and $<-0.5\,^{\circ}$C for Pasquill-Gifford classes G, F, E, and D, respectively. This area corresponds to Sutton Park Nature Reserve (Figure 1) which is the largest area of green space in Birmingham covering over 9.5 km^2. Sutton Park is approximately 40 m higher than the city centre and accounts for 70% of the outliers shown in Figure 7. Significant temperature gradients are also evident on the western edge of the city extents. These represent the remaining 30% of the outliers in Figure 7 and are caused by a distinct change to an increasingly rural environment containing Sandwell Valley Nature Reserve as well as numerous golf courses and farms. One particular feature of note is Woodgate Valley Country Park (Figure 1) which is effectively a green corridor running out to rural Worcestershire. Here, the closely spaced contour lines delineate a strong temperature gradient between the park and surrounding urban areas. This difference in temperature is particularly noticeable as the southern extents of the park are bordered by a dense urban (as defined by the (Owen *et al*., 2006) landuse classification) area. Further south there is another strong temperature gradient, explained by more parks, farms, and reservoirs.

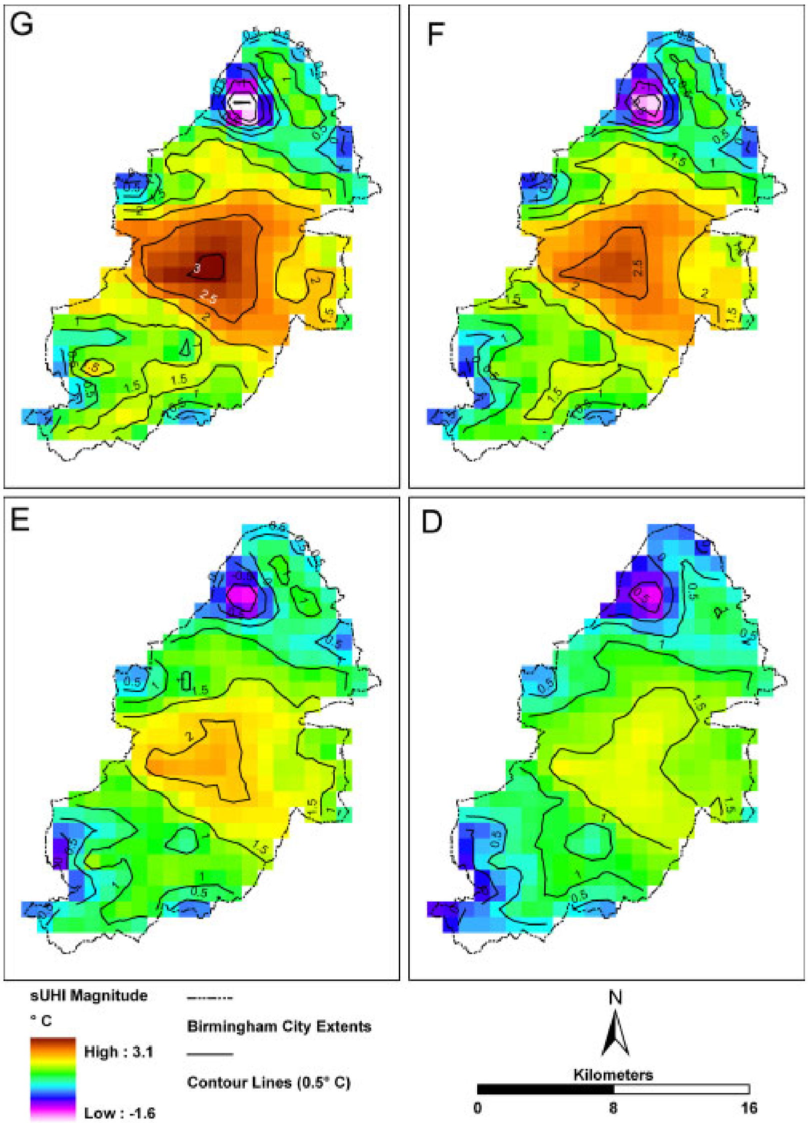

Figure 6. sUHI magnitude within Birmingham city extents across Pasquill-Gifford stability classes D, E, F, and G, shown with 0.5 °C contour lines. This figure is available in colour online at wileyonlinelibrary.com/journal/joc

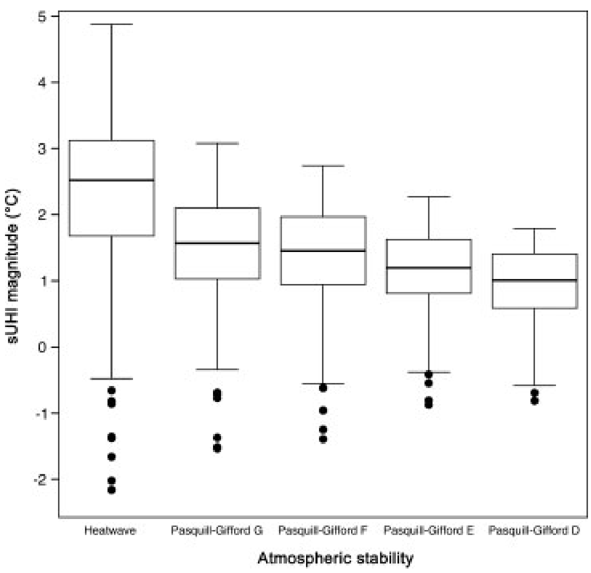

Figure 7. Boxplots of sUHI magnitude (°C) for different atmospheric stabilities.

3.3. Heatwave case study

The Local Climate Impacts Profile (LCLIP) report (Kotecha *et al*., 2008) for Birmingham is a database of weather events and consequences at a local scale collated from media reports (UKCIP, 2009). The database identifies various days as 'heatwave' events and during the study period, 4 heatwave events totalling 11 days were identified. Based on this reference, the LCLIP heatwave case study in July 2006 is used as a comparison 'extreme event' and the image for 18 July 2006 was processed using the described techniques (excluding any averaging) to make a fifth scenario for comparison alongside the four Pasquill-Gifford classes.

As illustrated in Figure 8, the averaged images discussed in the previous section can significantly hide the true magnitude of the heat island. Investigating a single image taken on 18 July 2006, in the early morning preceding a 'heatwave' day, a similar trend is seen. The contour mapping (Figure 8) shows the same spatial

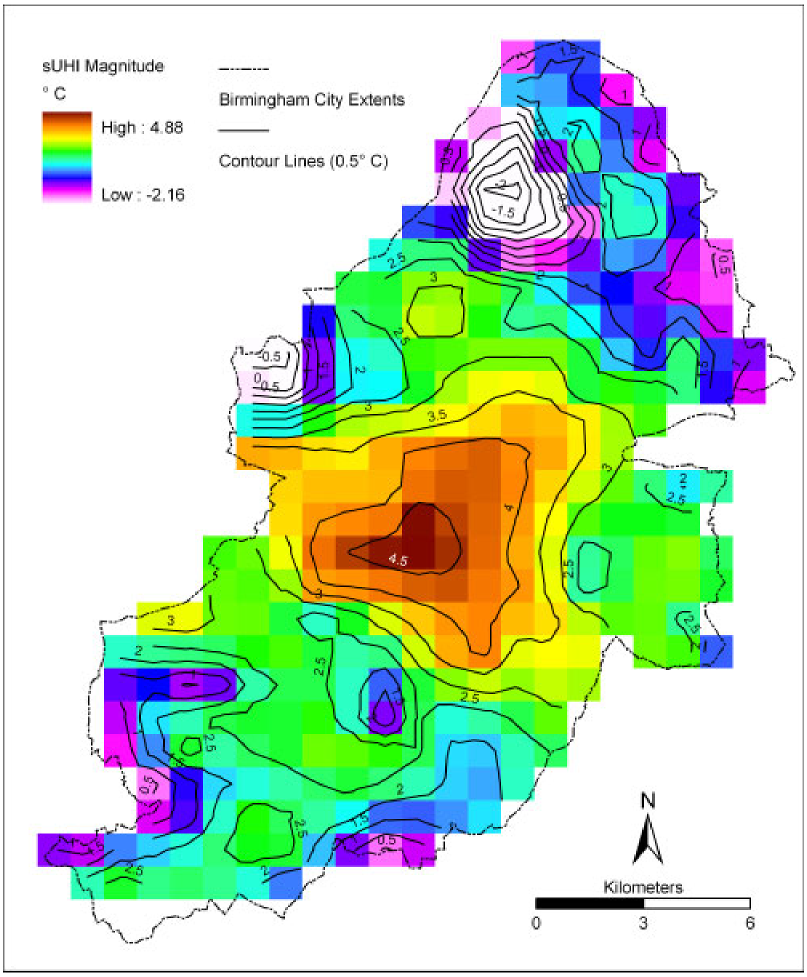

Figure 8. sUHI magnitude within Birmingham city extents for heatwave event (18 July 2006), shown with 0.5 °C contour lines. This figure is available in colour online at wileyonlinelibrary.com/journal/joc

trends already discussed, but with a greater temperature magnitude. The UHI magnitude peak in the centre is >4.5 °C, over 1.5 °C higher than the 'Extremely Stable' Pasquill-Gifford stability class G. A significant cold spot is again seen around Sutton Park, and at the western and southwestern city extents. This suggests that an increase in temperatures does not significantly alter the position of the UHI, but does increase the magnitude of both the UHI and the Sutton Park cold spot. It is interesting to note that the values (Table III) for a heatwave event are more than double the values for class E, the dominant stability class used in this study.

3.4. Thermal heterogeneity and landuse

Comparing UHI magnitude across different Pasquill-Gifford stability class by landuse (Figure 9) shows that in all cases except one, identical trends exist. Mean UHI magnitude increases across landuse classes in the order: 8 (woodland/open land), 3 (light suburban), 1 (villages/farms), 7 (light urban/open water), 2 (suburban), 4 (dense suburban), 6 (urban), and finally 5 (urban/transport). The only minor exception is for class D, where the mean values for 1 (villages/farms) and 7 (light urban/open water) switch places and is a likely consequence of the small number of pixels (Figure 4) categorised as class 7 (light urban/open water).

Indeed, when applying the Owens landuse class across Birmingham (Figure 4), over 80% of the landuse is explained by just 4 categories: (2 (suburban), 6 (urban), 4 (dense suburban), and 5 (urban/transport)). This is not surprising, considering that the classification is an urban classification and the study area is a major urban area. However, it is hard to draw any solid conclusions when considering groups 7 (light urban/open water) and 8 (woodland/open land) as they each make up <2% of Owens classification in Birmingham.

To test for statistical differences between UHI magnitudes and different landuse classes, Kruskal Wallis rank order tests were used with *post-hoc* Wilcoxon rank-sum tests. The results of the Kruskal Wallis rank order tests confirm that significant differences ($p < 0.05$) in UHI magnitude exist between at least two of the landuse classes in every scenario. The *post-hoc* Wilcoxon rank-sum tests show that significant differences ($p < 0.05$) exist between a number of landuses for each scenario, when using an appropriate Bonferroni correction factor. When using a correction factor, care must be taken in the

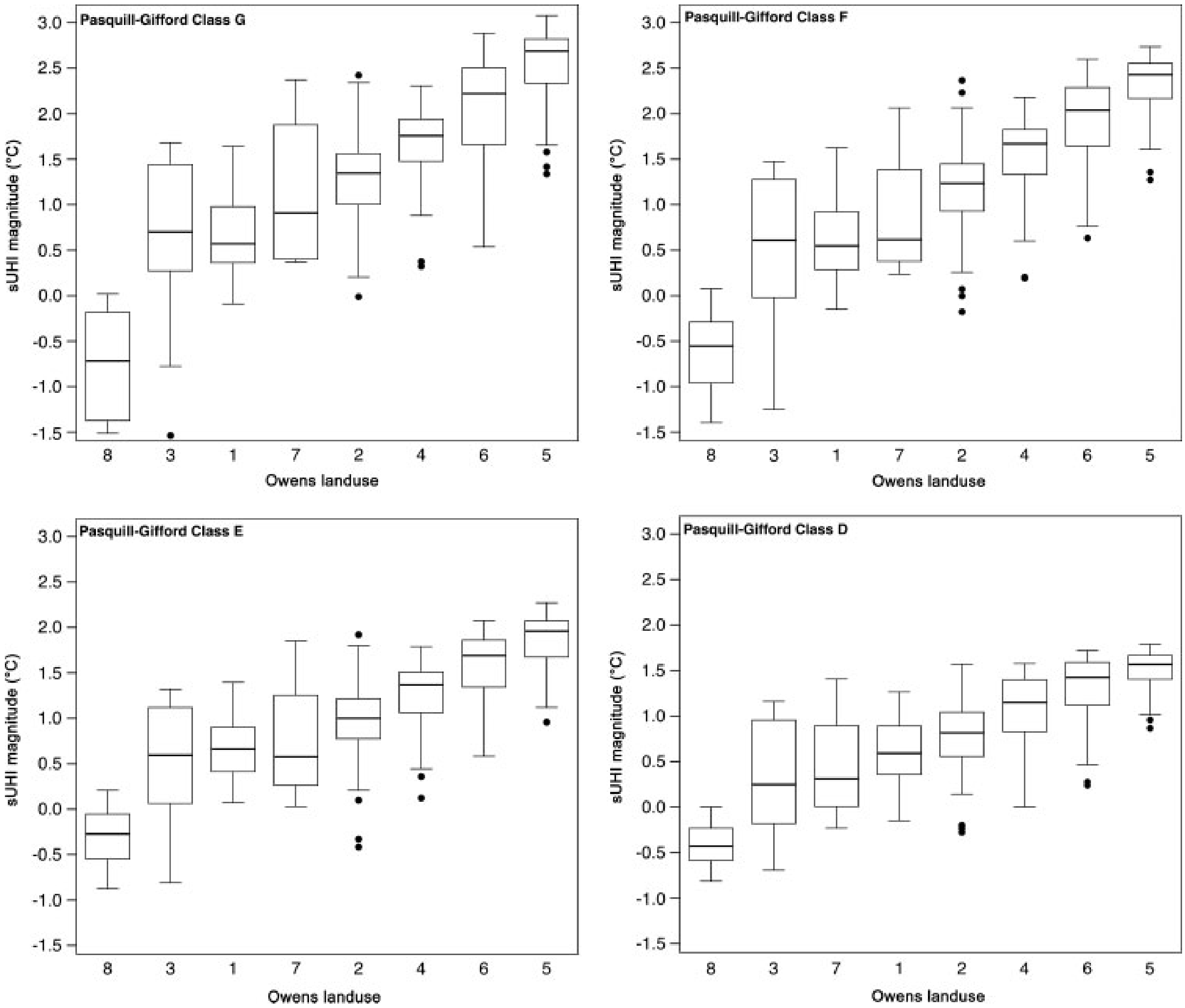

Figure 9. sUHI Magnitude for each Pasquill-Gifford class, distributed by Owens land and plotted in order of ascending mean sUHI magnitude. 1 (villages/farms), 2 (suburban), 3 (light suburban), 4 (dense suburban), 5 (urban/transport), 6 (urban), 7 (light urban/open water), 8 (woodland/open land).

interpretation as it becomes easy to reject results, potentially incorrectly. A summary of *post-hoc* test results (Table IV.) is split between the full landuse database and a partial landuse database, removing classes 7 (light urban/open water) and 8 (woodland/open land) due to the low sample count (Figure 4). The results change considerably as class 7 was showing most of the non-statistically significant change. In all scenarios, there is no statistical difference between landuse 1 (villages/farms) and 3 (light suburban), but this is understandable given the clear similarities between classes detailed in (Owen *et al*., 2006).

Table IV. Summary of *post-hoc* Wilcoxon rank-sum tests between landuse classes.

	Percentage of statistically significant results ($p < 0.05$) between landuse comparisons	
	Complete landuse (classes 1–8)	Partial landuse (classes 1–6)
	Bonferroni correction factor = 0.0018	Bonferroni correction factor = 0.0033
D (%)	60.71	80.00
E (%)	67.86	93.33
F (%)	67.86	93.33
G (%)	67.86	93.33
Heatwave	64.29	86.67

4. Conclusions

The surface night UHI of Birmingham has been shown to have considerable variation both spatially and across different levels of atmospheric stability. It has further been shown that landuse has a significant link to UHI magnitude. The averaged images clearly show a difference in UHI magnitude under different weather conditions, but the importance of investigating specific case studies such as the heatwave event of July 2006 is clearly demonstrated in this paper. Such extreme events could have significant consequences, for example, in the health-care sector. They are also likely to increase with climate change. However, when dealing with health impacts, it is ambient temperatures that are more important than surface temperatures. Indeed, a significant research gap that still exists is the relationship between measured surface LST such as used in this study, and air temperature. This is usually calculated by means of an empirical relationship, but in order for this to happen in the Birmingham study area data is required from a wider network of air temperature sensors than is presently available. It is hoped that in the future more work can be done on this relationship. Other future work could compare this MODIS dataset with Landsat ETM+ data, of higher spatial resolution but lower temporal resolution, to try and resolve temperature changes at a finer scale.

Overall, with the increasing interest in climate change adaptation within academia and at a policy level, the growing use of climate change models, and a rapidly rising urban population, there is a growing requirement for accurate high spatial and temporal resolution data relating to the UHI. This study has shown the utility of MODIS in providing a basic appraisal of the UHI magnitude which is suitable for these growing requirements, including UHI model verification and spatial risk assessment work. The study is significant for several reasons. Many previous UHI studies have focussed on 'ideal conditions' in megacities such as London or New York. This study differs from these in terms of the variety of meteorological conditions assessed as well as the size of the city under study (Birmingham can be seen as representative of many mid-latitude cities worldwide). Ultimately, this paper has presented a repeatable methodology for studying the UHI of individual conurbations that can be used worldwide with minimal adaptation, regardless of existing surface datasets.

Acknowledgements

This research has been funded by a Doctoral Training Award issued by the Engineering and Physical Sciences Research Council and supported by Birmingham City Council. It would not have been possible without data from both NASA and the UK Met Office. The satellite data is distributed by the Land Processes Distributed Active Archive Center (LP DAAC), located at the U.S. Geological Survey (USGS) Earth Resources Observation and Science (EROS) Center (lpdaac.usgs.gov). The weather station data is distributed by the British Atmospheric Data Centre (BADC) (badc.nerc.ac.uk). Thanks to Jason Roberts (Duke University) for his help with using the MGET plugin.

References

Arnfield AJ. 2003. Two decades of urban climate research: a review of turbulence, exchanges of energy and water, and the urban heat island. *International Journal of Climatology* **23**: 1–26, DOI:10.1002/joc.859.

Arnfield AJ. 2005. Micro- and mesoclimatology. *Progress in Physical Geography* **29**: 426–437, DOI:10.1191/0309133305pp458pr.

Arnfield AJ. 2006. Micro- and mesoclimatology. *Progress in Physical Geography* **30**: 677–689, DOI:10.1177/0309133306071150.

Basu R, Samet JM. 2002. Relation between elevated ambient temperature and mortality: a review of the epidemiologic evidence. *Epidemiologic Reviews* **24**: 190–202, DOI:10.1093/epirev/mxf007.

Bradley A, Thornes J, Chapman L, Unwin D, Roy M. 2002. Modelling spatial and temporal road thermal climatology in rural and urban areas using a GIS. *Climate Research* **22**: 41–55, DOI:10.3354/cr022041.

Burt S. 2004. The August 2003 heatwave in the United Kingdom: Part 1-Maximum temperatures and historical precedents. *Weather* **59**: 199–208, DOI:10.1256/wea.10.04A.

Changnon S, Kunkel K, Reinke B. 1995. Impacts and responses to the 1995 heat wave: A call to action. *Bulletin of the American Meteorological Society* **77**: 1497–1505, DOI:10.1175/1520-0477(1996)077<1497:IARTTH>2.0.CO;2.

Chapman L, Thornes J, Bradley A. 2001. Modelling of road surface temperature from a geographical parameter database. Part 1: Statistical. *Meteorological Applications* **8**: 409–419, DOI:10.1017/S1350482701004030.

Cheval S, Dumitrescu A. 2009. The July urban heat island of Bucharest as derived from MODIS images. *Theoretical and Applied Climatology* **96**: 145–153, DOI:10.1007/s00704-008-0019-3.

Cheval S, Dumitrescu A, Bell A. 2009. The urban heat island of Bucharest during the extreme high temperatures of July 2007. *Theoretical and Applied Climatology* **97**: 391–401, DOI:10.1007/s00704-008-0088-3.

Coll C, Caselles V, Galve J, Valor E, Niclos R, Sanchez J, Rivas R. 2005. Ground measurements for the validation of land surface temperatures derived from AATSR and MODIS data. *Remote Sensing of Environment* **97**: 288–300, DOI:10.1016/j.rse.2005.05.007.

Conti S, Meli P, Minelli G, Solimini R, Toccaceli V, Vichi M, Beltrano C, Perini L. 2005. Epidemiologic study of mortality during the Summer 2003 heat wave in Italy. *Environmental Research* **98**: 390–399, DOI:10.1016/j.envres.2004.10.009.

Gallo K, Tarpley J, McNab A, Karl T. 1995. Assessment of urban heat islands: a satellite perspective. *Atmospheric Research* **37**: 37–43, DOI:10.1016/0169-8095(94)00066-M.

Gawith M, Street R, Westaway R, Steynor A. 2009. Application of the UKCIP02 climate change scenarios: Reflections and lessons learnt. *Global Environmental Change* **19**: 113–121, DOI:10.1016/j.gloenvcha.2008.09.005.

Gedzelman S, Austin S, Cermak R, Stefano N. 2003. Mesoscale aspects of the urban heat island around New York City. *Theoretical and Applied Climatology* **75**: 29–42, DOI:10.1007/s00704-002-0724-2.

Giridharan R, Kolokotroni M. 2009. Urban heat island characteristics in London during winter. *Solar Energy* **83**: 1668–1682, DOI:10.1016/j.solener.2009.06.007.

Greater London Authority. 2006. *London's Urban Heat Island: A Summary for Decision Makers*.

Huang H, Ooka R, Kato S. 2005. Urban thermal environment measurements and numerical simulation for an actual complex urban area covering a large district heating and cooling system in summer. *Atmospheric Environment* **39**: 6362–6375, DOI:10.1016/j.atmosenv.2005.07.018.

Hung T, Uchihama D, Ochi S, Yasuoka Y. 2006. Assessment with satellite data of the urban heat island effects in Asian mega cities. *International Journal of Applied Earth Observation and Geoinformation* **8**: 34–48, DOI:10.1016/j.jag.2005.05.003.

Jenkins GJ, Murphy JM, Sexton DS, Lowe JA, Jones P, Kilsby CG. 2009. *UK Climate Projections: Briefing report*. Met Office Hadley Centre: Exeter, UK.

Jin M, Dickinson R, Zhang D. 2005. The footprint of urban areas on global climate as characterized by MODIS. *Journal of Climate* **18**: 1551–1565, DOI:10.1175/JCLI3334.1.

Jin M, Shepherd JM. 2005. Inclusion of Urban Landscape in a Climate Model: How Can Satellite Data Help? *Bulletin of the American Meteorological Society* **86**: 681–689, DOI:10.1175/BAMS-86-5-681.

Johnson D. 1985. Urban modification of diurnal temperature cycles in Birmingham, U.K. *International Journal of Climatology* **5**: 221–225, DOI:10.1002/joc.3370050208.

Jones PD, Lister DH. 2009. The urban heat island in Central London and urban-related warming trends in Central London since 1900. *Weather* **64**: 323–327, DOI:10.1002/wea.432.

Karl T, Diaz H, Kukla G. 1988. Urbanization: Its detection and effect in the United States climate record. *Journal of Climate* **1**: 1099–1123, DOI:10.1175/1520-0442(1988)001<1099:UIDAEI>2.0.CO;2.

Kolokotroni M, Zhang Y, Watkins R. 2007. The London Heat Island and building cooling design. *Solar Energy* **81**: 102–110, DOI:10.1016/j.solener.2006.06.005.

Kolokotroni M, Giridharan R. 2008. Urban heat island intensity in London: An investigation of the impact of physical characteristics on changes in outdoor air temperature during summer. *Solar Energy* **82**: 986–998, DOI:10.1016/j.solener.2008.05.004.

Kotecha R, Thornes J, Chapman L. 2008. *Birmingham's Local Climate Impacts Profile (LCLIP)*.

Kukla G, Gavin J, Karl T. 1986. Urban warming. *Journal of Applied Meteorology* **25**: 1265–1270, DOI:10.1175/1520-0450(1986) 025<1265:UW>2.0.CO;2.

Lindley SJ, Handley JF, Theuray N, Peet E, McEvoy D. 2006. Adaptation Strategies for Climate Change in the Urban Environment: Assessing Climate Change Related Risk in UK Urban Areas. *Journal of Risk Research* **9**: 543–568, DOI:10.1080/13669870600798020.

Matson M, Mcclain E, McGinnis Jr D, Pritchard J. 1978. Satellite detection of urban heat islands. *Monthly Weather Review* **106**: 1725–1734, DOI:10.1175/1520-0493(1978)106<1725: SDOUHI> 2.0.CO;2.

Mckendry IG. 2003. Applied climatology. *Progress in Physical Geography* **27**: 597–606, DOI:10.1191/0309133303pp397pr.

Mendelsohn R, Kurukulasuriya P, Basist A, Kogan F, Williams C. 2007. Climate analysis with satellite versus weather station data. *Climatic Change* **81**: 71–83, DOI:10.1007/s10584-006-9139-x.

Met Office. 2010. *UK Climate Summaries.* Accessed: Feb 2010. http://www.metoffice.gov.uk/climate/uk/.

Morris C, Simmonds I, Plummer N. 2001. Quantification of the influences of wind and cloud on the nocturnal urban heat island of a large city. *Journal of Applied Meteorology* **40**: 169–182, DOI:10.1175/1520-0450(2001)040<0169:QOTIOW>2.0.CO;2.

NASA Land Processes Distributed Active Archive Center. 2009. *MODIS/Aqua Land Surface Temperature and Emissivity Daily L3 Global 1 km Grid SIN.* Accessed: Jan 2010. https://lpdaac.usgs.gov/lpdaac/products/modis_products_table/land_surface_temperature_emissivity/daily_l3_global_1 km/myd11a1.

Nichol JE. 1994. A GIS-Based Approach to Microclimate Monitoring in Singapore's High-Rise Housing Estates. *Photogrammetric Engineering & Remote Sensing* **60**: 1225–1232.

Office for National Statistics. 2009. *Key Population and Vital Statistics 2007.* Accessed: Jan 2010. http://www.statistics.gov.uk/StatBase/Product.asp?vlnk=539.

Oke TR. 1987. *Boundary Layer Climates Second Edition.* Routledge: London and New York.

Owen S, MacKenzie A, Bunce R, Stewart H, Donovan R, Stark G, Hewitt C. 2006. Urban land classification and its uncertainties using principal component and cluster analyses: A case study for the UK West Midlands. *Landscape and Urban Planning* **78**: 311–321, DOI:10.1016/j.landurbplan.2005.11.002.

Pasquill F, Smith FB. 1983. *Atmospheric Diffusion Third Edition.* Ellis Horwood Limited: Chichester.

Pongracz R, Bartholy J, Dezso Z. 2006. Remotely sensed thermal information applied to urban climate analysis. *Advances in Space Research* **37**: 2191–2196, DOI:10.1016/j.asr.2005.06.069.

Price J. 1979. Assessment of the urban heat island effect through the use of satellite data. *Monthly Weather Review* **107**: 1554–1557, DOI:10.1175/1520-0493(1979)107<1554:AOTUHI>2.0.CO;2.

Rajasekar U, Weng Q. 2008. Urban heat island monitoring and analysis using a non-parametric model: A case study of Indianapolis. *ISPRS Journal of Photogrammetry and Remote Sensing* **64**: 86–96, DOI:10.1016/j.isprsjprs.2008.05.002.

Rigo G, Parlow E, Oesch D. 2006. Validation of satellite observed thermal emission with in-situ measurements over an urban surface. *Remote Sensing of Environment* **104**: 201–210, DOI:10.1016/j.rse.2006.04.018.

Rizwan A, Dennis L, Liu C. 2008. A review on the generation, determination and mitigation of Urban Heat Island. *Journal of Environmental Sciences* **20**: 120–128, DOI:10.1016/S1001-0742(08)60019-4.

Roberts JJ, Best BD, Dunn DC, Treml EA, Halpin PN. 2010. Marine Geospatial Ecology Tools: An integrated framework for ecological geoprocessing with ArcGIS, Python, R, MATLAB, and C++. *Environmental Modelling & Software* **25**: 1197–1207, DOI: 10.1016/j.envsoft.2010.03.029.

Rooney C, Mcmichael AJ, Kovats RS, Coleman MP. 1998. Excess mortality in England and Wales, and in Greater London, during the 1995 heatwave. *Journal of Epidemiology & Community Health* **52**: 482–486, DOI:10.1136/jech.52.8.482.

Sarrat C, Lemonsu A, Masson V, Guedalia D. 2006. Impact of urban heat island on regional atmospheric pollution. *Atmospheric Environment* **40**: 1743–1758, DOI:10.1016/j.atmosenv.2005.11.037.

Smith C, Lindley S, Levermore G. 2009. Estimating spatial and temporal patterns of urban anthropogenic heat fluxes for UK cities: the case of Manchester. *Theoretical and Applied Climatology* **98**: 19–35, DOI:10.1007/s00704-008-0086-5.

Souch C, Grimmond S. 2006. Applied climatology: urban climate. *Progress in Physical Geography* **30**: 270–279, DOI:10.1191/0309133306pp484pr.

Stabler L, Martin C, Brazel A. 2005. Microclimates in a desert city were related to land use and vegetation index. *Urban Forestry & Urban Greening* **3**: 137–147, DOI:10.1016/j.ufug.2004.11.001.

Streutker D. 2003. Satellite-measured growth of the urban heat island of Houston, Texas. *Remote Sensing of Environment* **85**: 282–289, DOI:10.1016/S0034-4257(03)00007-5.

Sutherland R, Hansen F, Bach W. 1986. A quantitative method for estimating Pasquill stability class from windspeed and sensible heat flux density. *Boundary-Layer Meteorology* **37**: 357–369, DOI:10.1007/BF00117483.

Svensson M. 2004. Sky view factor analysis–implications for urban air temperature differences. *Meteorological Applications* **11**: 201–211, DOI:10.1017/S1350482704001288.

Torok S, Morris C, Skinner C, Plummer N. 2001. Urban heat island features of southeast Australian towns. *Australian Meteorological Magazine* **50**: 1–13.

UK Meteorological Office. 2006. *MIDAS Land Surface Stations data (1853-current), [Internet].* Accessed: Jan 2010. http://badc.nerc.ac.uk/data/ukmo-midas.

UKCIP. 2009. *A local climate impacts profile: how to do an LCLIP.* UKCIP: Oxford.

Unger J. 2004. Intra-urban relationship between surface geometry and urban heat island: review and new approach. *Climate Research* **27**: 253–264, DOI:10.3354/cr027253.

Unger J. 2006. Modelling of the annual mean maximum urban heat island using 2D and 3D surface parameters. *Climate Research* **30**: 215–226, DOI:10.3354/cr030215.

Unwin DJ. 1980. The Synoptic Climatology of Birmingham's Urban Heat Island, 1965-74. *Weather* **35**: 43–50.

Wan Z. 1999. *MODIS Land-Surface Temperature Algorithm Theoretical Basis Document (LST ATBD).* University of California, Santa Barbara, USA: Institute for Computational Earth System Science. Accessed: Jan 2010. http://modis.gsfc.nasa.gov/data/atbd/atbd_mod11.pdf.

Wan Z. 2002. Validation of the land-surface temperature products retrieved from Terra Moderate Resolution Imaging Spectroradiometer data. *Remote Sensing of Environment* **83**: 163–180, DOI:10.1016/S0034-4257(02)00093-7.

Wan Z. 2008. New refinements and validation of the MODIS Land-Surface Temperature/Emissivity products. *Remote Sensing of Environment* **112**: 59–74, DOI:10.1016/j.rse.2006.06.026.

Wan Z, Dozier J. 1996. A generalized split-window algorithm for retrieving land-surface temperature from space. *IEEE Transactions on Geoscience and Remote Sensing* **34**: 892–905, DOI:10.1109/36.508406.

Wan Z, Zhang Y, Zhang Q, Li Z. 2004. Quality assessment and validation of the MODIS global land surface temperature. *International Journal of Remote Sensing* **25**: 261–274, DOI:10.1080/0143116031000116417.

Watkins R, Palmer J, Kolokotroni M. 2002. The London Heat Island: results from summertime monitoring. *Building Services Engineering Research and Technology* **23**: 97–106, DOI:10.1191/0143624402bt031oa.

Weller J, Thornes J. 2001. An investigation of winter nocturnal air and road surface temperature variation in the West Midlands, UK under different synoptic conditions. *Meteorological Applications* **8**: 461–474, DOI:10.1017/S1350482701004078.

Weng Q. 2009. Thermal infrared remote sensing for urban climate and environmental studies: Methods, applications, and trends. *ISPRS Journal of Photogrammetry and Remote Sensing* **64**: 335–344, DOI:10.1016/j.isprsjprs.2009.03.007.

Wilby R. 2003. Past and projected trends in London's urban heat island. *Weather* **58**: 251–260, DOI:10.1256/wea.183.02.

